



ELSEVIER

Seminars in

ROENTGENOLOGY

The Elbow: Radiographic Imaging Pearls and Pitfalls

David E. Grayson, MD, Major, USAF, MC

Diagnostic imaging of the elbow has seen remarkable advances in the last several years. The multiplanar capabilities and increasing availability of magnetic resonance (MR) and volumetric multislice computed tomographic (CT) imaging allow exquisitely detailed imaging of the osseous and articular components of the elbow. In addition, MR imaging, with its superior soft-tissue contrast, is optimally suited to evaluate the supporting soft-tissue structures and articular cartilage, without the use of ionizing radiation.^{1,2} Sonography has also shown promise in the evaluation of soft tissues, articular surfaces, detection of loose bodies, and in the diagnosis and healing of fractures.^{1,3} However, despite these advances in elbow imaging, conventional radiography remains the most appropriate initial imaging technique of the elbow and its disorders.^{1,2} This review focuses on the typical radiographic findings associated with several clinical entities that one may expect to see in daily clinical practice. The indications for and imaging features of more advanced complementary modalities are also briefly discussed.

Anatomy

The elbow articulation is made up of three highly congruous joint surfaces and is considered a trochoglymoid joint.⁴ The trochoid (pivoting) components consist of the radiohumeral and proximal radioulnar joints, which allow for axial rotation of the forearm. The ginglymus (hinge) component is created by the ulnohumeral joint, allowing for flexion and extension. Full hinge motion is assisted by the deep invaginations of the distal humeral olecranon and coronoid fossae. During elbow development, four separate

distal humeral ossification centers form. Although the sequence of ossification may vary, the lateral epicondyle, capitellum, and trochlea are united to form a single epiphysis in approximately the 13th year, which then fuses to the humeral shaft around age 16.⁵ The medial epicondylar epiphysis is extraarticular and remains open into the late teens.⁵ The capitellum ossification center will appear earliest, always by 2 years of age, followed closely by that of the radial head. Dual or multiple ossification centers are commonly seen within the trochlea and olecranon epiphyses.⁵ The sequential order of appearance of the ossification centers of the elbow can be remembered by the mnemonic "CRITOE": capitellum, radial head, internal or medial epicondyle, trochlea, and external or lateral epicondyle.

Static stabilizers of the elbow include the thin joint capsule and supporting collateral ligaments. Extrasynovial anterior and posterior fat pads are located deep to the capsular margins.⁴ Bursae form over the olecranon process (superficial olecranon bursa) and between the distal biceps tendon and the tuberosity of the radius (bicipitoradial bursa).

Radiography

A routine radiographic evaluation of the elbow includes an anteroposterior (AP) and true lateral view.^{1,2} For the AP view the elbow should be fully extended with the forearm supinated (Fig. 1A), allowing optimal visualization of the medial and lateral epicondyles, radiocapitellar joint, and estimation of the carrying angle (the angle formed between the longitudinal axes of the humerus and the forearm on AP projection, normally between 11 and 13° of valgus).^{6,7} The lateral view should be obtained with the elbow in 90° of flexion and the forearm in neutral (thumb up) position (Fig. 1B).⁷ A true lateral radiograph allows a "teardrop" appearance to be formed by the boundaries of the coronoid and olecranon fossae.⁸ The ulnotrochlear joint, coronoid process, and olecranon process are well seen in this projection. In the setting of trauma or arthrosis, additional oblique radiographs may be of benefit. The lateral oblique view is similar to the AP except that the hand and forearm are fully externally rotated. The standard lateral view may also be optimized to evaluate the radial head by having the

Academic Chief, Musculoskeletal Section, Department of Radiology—Wilford Hall Medical Center, Lackland AFB, TX; and Adjunct Assistant Professor of Radiology/Radiological Sciences, Uniformed Services University of the Health Sciences, F. Edward Herbert School of Medicine, Bethesda, MD.

The opinions and assertions contained herein are those of the authors and should not be construed as official or as representing the opinions of the Department of the Air Force or the Department of Defense.

Address reprint requests to David E Grayson, MD, Academic Chief, Musculoskeletal Section, Department of Radiology—Wilford Hall Medical Center, 759 MDTs/MTRD, 2200 Bergquist Drive, Suite 1, Lackland AFB, TX 78236-5300. E-mail: David.grayson@lackland.af.mil

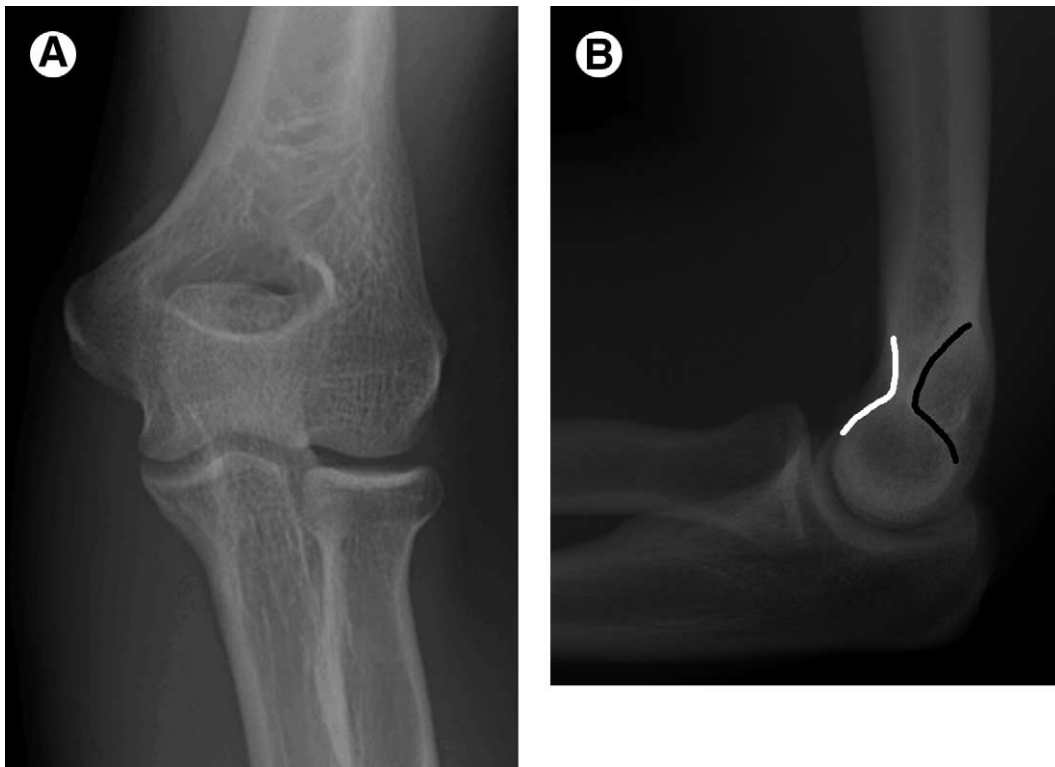


Figure 1 Standard views. Anteroposterior (A) and lateral (B) elbow views are demonstrated. Anteroposterior view is obtained during full elbow extension with forearm supinated. Radiocapitellar joint and epicondylar margins are well seen. Lateral view is obtained with elbow in 90° of flexion and forearm in neutral position. Note “teardrop” formed by coronoid (white line) and olecranon (black line) fossae when elbow is well positioned.

tube angled 45° cephalically along the humeral shaft.⁷ The importance of obtaining well-positioned diagnostic radiographs cannot be overemphasized. This can be especially difficult when attempting to image an injured child.

Table 1 is a checklist of the important landmarks in the radiographic evaluation of the elbow.

Table 1 Radiographic Evaluation of the Elbow Joint

Anterior humeral line passes through middle third of capitellum
Radiocapitellar line passes through capitellum on every radiographic view
Coronoid line should be smooth and concave
Check for abnormal fat pads
Elevated anterior fat pad or sail sign
Visible posterior fat pad
Displaced supinator fat plane
Olecranon bursa
Ossification centers, “CRITOE”
Capitellum
Radial head
Internal or medial epicondyle
Trochlea
Olecranon
External or lateral epicondyle

Trauma

Depending on the injury mechanism and degree of force, characteristic fracture and dislocation patterns occur in and around the elbow. Non-displaced or minimally displaced fractures may not be readily visualized on initial radiographs. However, a high index of suspicion and knowledge of relevant radiographic anatomy and secondary signs of injury will prove useful.

Fat Pad Sign

As noted previously, extra-synovial fatty collections are present within the capsular margins of the elbow joint. The posterior fat pad normally lies deep within the olecranon fossa. Any process that distends the joint (hematoma in the setting of trauma) will push the radiolucent fat out beyond the borders of the posterior humeral cortex on the lateral view (Fig. 2A).^{5,9,10} The anterior fat pad is normally visible as a thin lucent arc anterior to the distal humeral cortex, but may become displaced anterosuperiorly and bulge convexly away from the joint, creating an anterior sail sign (Fig. 2A).¹⁰ An occult fracture is likely to be present in the setting of elbow effusion without a radiographically visualized fracture (Fig. 2B).^{11,12} The presence of a fat pad sign is especially important in pediatric



Figure 2 Fat pad sign. Lateral view (A) shows displacement of anterior (white arrows) and posterior (black arrow) extra-synovial fat pads, indicating distension of the joint capsule. (B) Lateral view in different child demonstrates anterior “sail” sign. Normally visible thin anterior fat pad has become elevated and displaced anteriorly like sail of a ship (white arrows). Non-displaced fracture of distal humerus is suggested by subtle disruption of anterior cortical margin (black arrow). Obliquely oriented supracondylar fracture is well seen and confirmed by MR imaging (C). Sagittal T1-weighted MR image demonstrates low signal serpentine course of fracture (arrows).

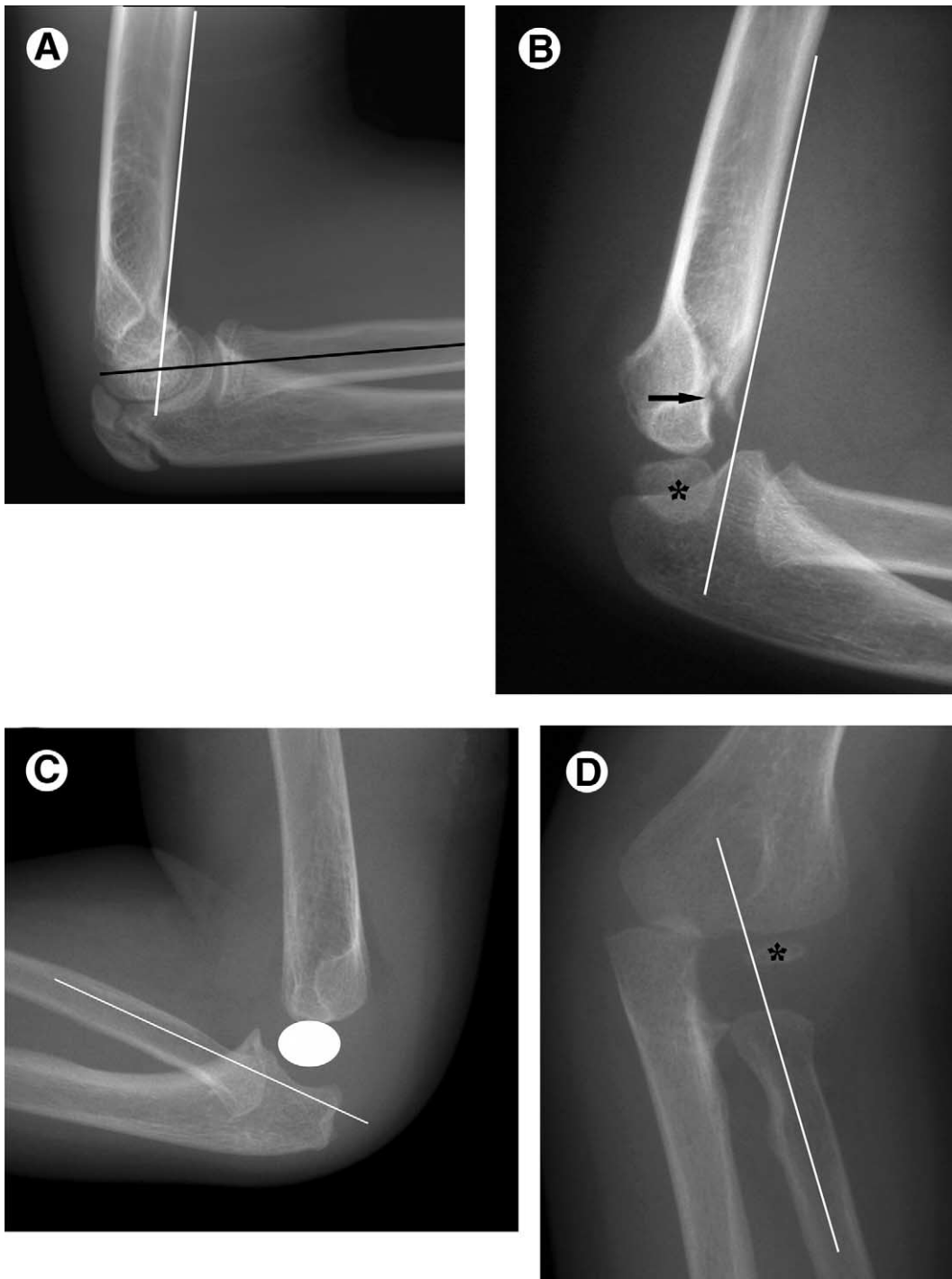


Figure 3 Anterior humeral and radio-capitellar lines. (A) Anterior humeral line (white line) is drawn along the anterior humeral margin of well-positioned lateral elbow view. Anterior humeral line should normally intersect the middle one-third of capitellum ossification center. Anterior or posterior displacement of capitellum suggests physeal injury or humeral supracondylar fracture. Additional line drawn along central long-axis of radius (black line) should intersect capitellum ossification center. This is the radio-capitellar line and can be reliably reproduced on any view, regardless of obliquity. Any deviation represents dislocation or subluxation of radial head. (B) Lateral view shows posterior displacement of capitellum ossification center (asterisk) relative to anterior humeral line (line) in setting of displaced supracondylar fracture (arrow). (C) Lateral view in different patient reveals posterior dislocation of radial head. Radio-capitellar line (line) passes well below expected location of capitellum ossification center (white ellipse). (D) Lateral oblique view demonstrates antero-medial subluxation of radial head. Radio-capitellar line (line) passes medial to capitellum ossification center (asterisk).



Figure 4 Childhood fractures. (A) Anteroposterior view demonstrates minimally displaced fracture through lateral condyle (arrow). This injury pattern is common in young children. (B) Lateral elbow view in different child shows posterior displacement of capitellum relative to anterior humeral line. Joint effusion is indicated by presence of both anterior (white arrow) and posterior (black arrow) fat pad signs. Incidentally noted is supracondylar process in distal humerus. (C) Anteroposterior view in same patient as (B) reveals buckling of medial supracondylar margin (arrow).

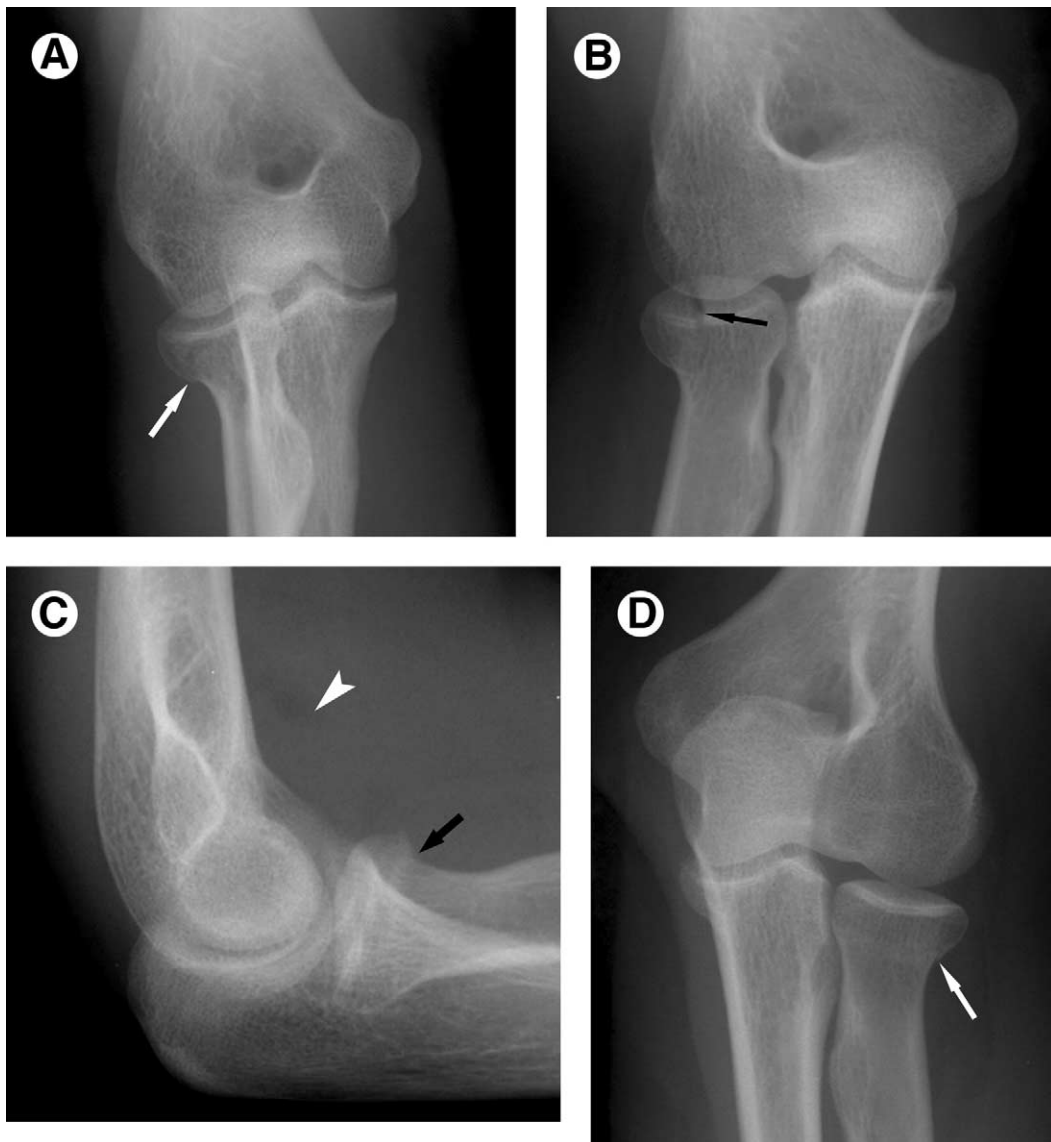


Figure 5 Radial head fractures. (A) Anteroposterior view reveals focal disruption of anterolateral cortical margin (arrow) in this patient with fracture of radial head. (B) Full intraarticular extent of fracture (arrow) is seen to better advantage with lateral oblique view. (C) Focal buckling of normally smooth concave margin of radial head and neck junction (black arrow) in different patient indicates fracture. Note displaced anterior fat pad (white arrow), resulting from joint effusion and capsular distension. (D) Subtle cortical disruption along lateral margin of radial neck (arrow) corresponds to non-displaced fracture in this patient following fall on outstretched hand.

cases where a fracture may involve only the immature cartilaginous components. In these cases, MR imaging with cartilage and marrow-sensitive sequences will best depict the fracture site and degree of displacement (Fig. 2C).^{2,8,11}

Anterior Humeral Line

A line drawn along the anterior humeral cortex on the lateral radiograph should normally intersect the middle one-third of the capitellum ossification center (Fig. 3A). Anterior or posterior positioning of the capitellum indicates either physeal injury with capitellar displacement or subtle fracture of the supracondylar portion of the distal

humerus (Fig. 3B).¹³ A true lateral projection is imperative as oblique views may result in a false-negative sign.

Radio-Capitellar Line

On any radiographic view, regardless of obliquity, a line drawn along the long axis of the radius should intersect with the capitellum (Fig. 3A).¹³ Any deviation suggests subluxation or frank dislocation of the radial head (Fig. 3C and D). Care should be taken to orient the line along the diaphysis of the radius rather than the proximal metaphysis, which normally has mild lateral angulation, to avoid a false-positive result.¹³

In children under 4 years of age, the weakest compo-

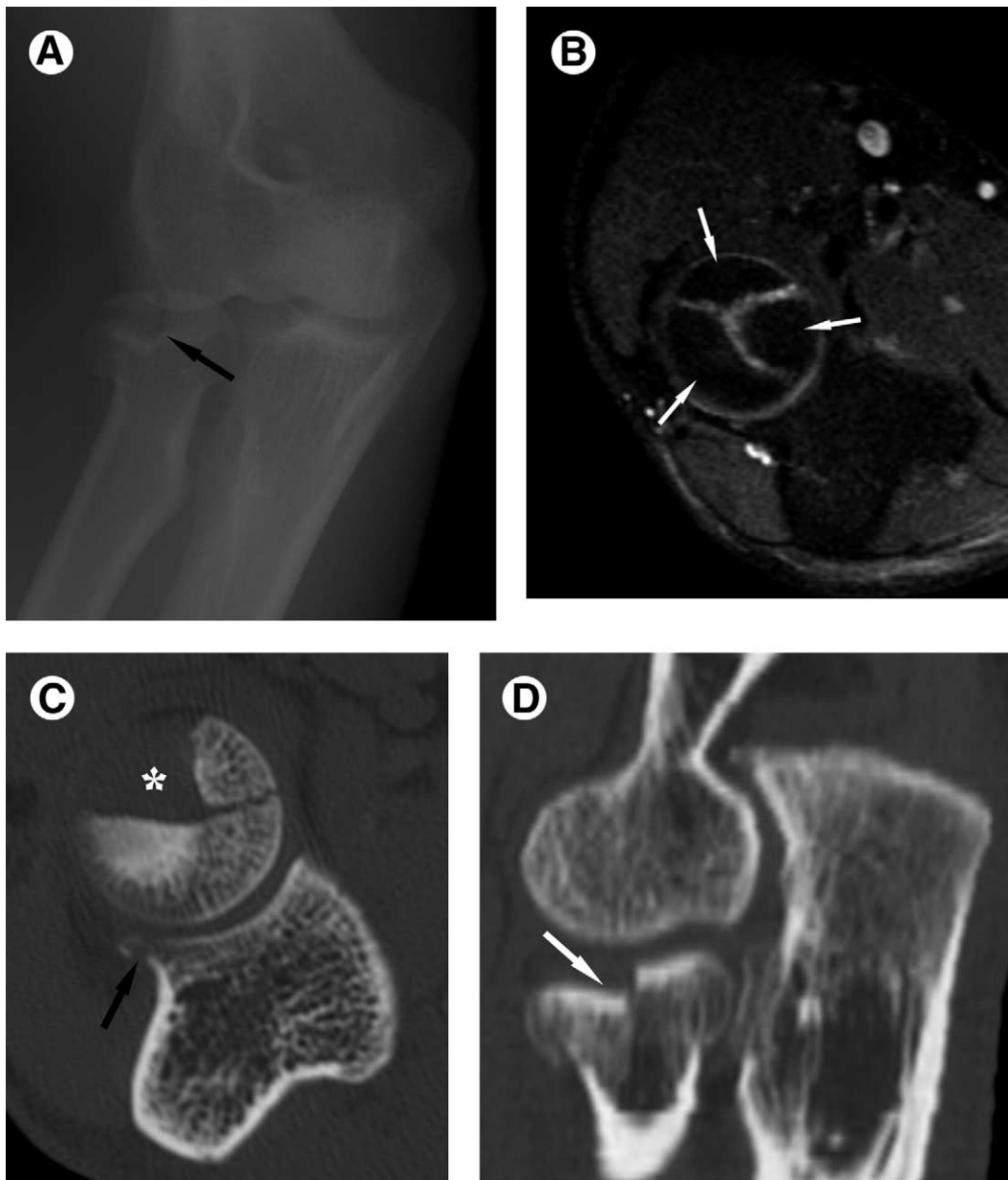


Figure 6 Comminuted fracture. (A) Lateral oblique view demonstrates intraarticular comminuted radial head fracture (arrow) with depressed anterior component. (B) Axial T2-weighted MR image with fat-saturation well shows comminuted components (arrows). Axial (C) and sagittal (D) reformatted CT images allow accurate evaluation of degree of comminution, displacement, and intraarticular step-off (asterisk, white arrow) of fracture fragments. Unsuspected minimally displaced fracture of proximal ulna is also well demonstrated (C, black arrow).

ment of the distal humerus is along the distal humeral epiphyseal growth plate. Horizontal shear injuries often result in Salter–Harris type I or II fractures.⁵ The capitellum ossifies as early as 6 months and always by 2 years, which serves as a useful landmark in young children for potentially displaced fractures through the distal humeral cartilage. Between the ages of 4 and 10 years, the physis is stronger than the distal humeral metaphysis. In these children 60% of elbow fractures are supracondylar followed by lateral and then medial condylar injuries (Fig. 4).^{5,14,15} It should be remembered that condyle fractures are often Salter–Harris type IV injuries, with intraarticular exten-

sion of the fracture across the physis, through the cartilaginous portions of trochlea or capitellum.¹⁴ Medial epicondylar avulsion fractures, occurring most often between the ages of 9 and 15 years, should be carefully sought following partial or complete elbow dislocation, especially after manual reduction.⁵ With regard to epicondylar physeal injury in older children, comparison with the contralateral elbow may be necessary to confirm subtle widening of the symptomatic physis.

In sharp contrast to the frequency of distal humeral fractures in children, radial head fractures (Fig. 5) account for approximately 50% of elbow fractures in adults, com-



Figure 7 Fracture-dislocation. (A) Anteroposterior view extended over proximal forearm shows severely comminuted fracture of ulnar midshaft (black arrows) with associated anterolateral dislocation of radial head (white arrow), first described by Monteggia. (B) Anteroposterior view in different patient reveals angulated fracture of radial shaft associated with disruption of distal radioulnar joint, consistent with Galeazzi fracture dislocation. Image contributed by Liem T. Bui-Mansfield, Brooke Army Medical Center, San Antonio, TX. (C) Anteroposterior view in different patient demonstrates impacted and angulated fracture of radial neck (arrowheads). This appearance indicates high-energy injury mechanism. Associated disruption of interosseous membrane and distal radioulnar joint (not shown) may occur, representing the fracture-dislocation of Essex-Lopresti.

monly following a fall on an outstretched hand with the forearm in pronation.^{16,17} This mechanism often impacts the anterolateral quadrant of the radial head and is associated with other soft-tissue injuries in up to 30% of cases, including joint dislocation. Any subtle exaggeration of cortical concavity along the radial head–neck junction represents a fracture (Fig. 5C and D), often seen on only one view. Lateral oblique or radial head views may be necessary to identify subtle non-displaced radial head fractures.^{16,18} Intraarticular step-off of greater than 2 mm or involvement of more than one-third of the radial head surface (Fig. 6) is strong indication for open reduction and internal fixation.¹⁹

The forearm is considered to be a ring structure similar to the pelvis. Consequently, when one of the forearm bones is fractured, it is common to have an associated dislocation or fracture of the other bone. There are three well-recognized fracture dislocation patterns involving the elbow and forearm. These are summarized in Table 2

Monteggia Fracture/Dislocation (Fig. 7A)

First described in 1814 by Giovanni Monteggia, this injury involves fracture of the ulnar shaft with associated dislocation of the radiocapitellar joint.²⁰ The ulnar fracture will show apex-medial angulation and the radial head often dislocates anteriorly.

Galeazzi Fracture/Dislocation (Fig. 7B)

First described in 1943 by Galeazzi, this injury involves an obvious oblique and displaced, with angulation, fracture of the radial shaft. However, the dislocation of the distal radioulnar joint may be subtle.

Essex-Lopresti Fracture/Dislocation (Fig. 7C)

A highly comminuted or impacted fracture of the radial head may be associated with dislocation of the distal radioulnar joint. The force of the injury is directed along the interosseous membrane of the forearm, which disrupts the distal radioulnar joint,²¹ as described by Essex-Lopresti.

Careful radiographic evaluation of the wrist and forearm should follow any elbow injury when patient's symptoms warrant.

After radial head and complex fracture dislocations, olecranon process fractures occur commonly in the adult (Fig. 8). The olecranon process is in a subcutaneous location, lending itself vulnerable to trauma, frequently presenting as a comminuted open fracture following high-impact injury while in the flexed position.¹⁶



Figure 8 Olecranon fracture. Lateral radiograph demonstrates transverse fracture of olecranon process with proximal retraction of major fragment (white arrow). Contraction of intact triceps brachii muscle-tendon unit greatly increases chance of nonunion if surgical fixation is not performed. Displaced coronoid process fracture (black arrow) and intraarticular radial head fracture (black arrowhead) are also present. Note displaced anterior fat pad (white arrowhead), indicating joint effusion.

Complete posterior dislocation of the elbow (Fig. 9) is always associated with injury to the ulnar collateral ligament¹⁹ and shearing fracture of the coronoid process is not uncommon.^{16,22} Untreated coronoid fractures predispose to recurrent dislocations and early secondary osteoarthritis.¹⁹

Postprocessing of volumetrically acquired CT images allows for three-dimensional rendering or multiplanar reformatting of complex fractures, thus aiding surgical planning for optimal reduction and fixation (Fig. 10A and B).¹ Routine CT imaging can also prove useful when adequate radiographic views cannot be obtained.²³ The judicious use of MR imaging will aid in confirming and characterizing complex or radiographically occult fractures with a high degree of sensitivity (Fig. 10C and D).²⁴ In addition, this technique allows evaluation of the integrity of the collateral ligaments, articular cartilaginous surfaces, and joint capsule.¹

Table 2 Summary of Fracture-Dislocation Patterns of the Forearm

Eponyms	Mnemonic	Fracture	Dislocation
Galeazzi	GRD	Radial shaft	Distal [DRUJ]
Essex-Lopresti	ERD	Radial head	Distal [DRUJ]
Monteggia	MUP	Ulna	Proximal [RCJ]

DRUJ = distal radioulnar joint; RCJ = radiocapitellar joint.



Figure 9 Complete elbow dislocation. (A) Anteroposterior and (B) lateral views demonstrate complete posterior and lateral dislocation of elbow. Several small avulsion fragments (arrows) are present. Coronoid process should be carefully evaluated following reduction, as untreated shear-type fracture will predispose to additional instability, recurrent dislocation, and early osteoarthritic change. (C) Sagittal T2-weighted MR image with fat-saturation in different patient demonstrates laxity and focal disruption of joint capsule (arrows) following complete dislocation. MR imaging is also useful in evaluation of collateral ligaments and articular surfaces.

The Young Athlete

The number of pediatric and adolescent throwing athletes being treated for elbow injuries is increasing as participation and competitive levels rise in the general population.²⁵ The mechanical forces of valgus extension overload during late cocking and early acceleration phases of throwing induce distractive forces on the medial joint and compressive forces on the lateral joint.^{6,26} Additional shear forces affect the radiocapitellar joint and olecranon process during late acceleration and deceleration phases. With overuse, age-dependent injury patterns may occur. Physeal injury and apophysitis occur in childhood, while epicondylar avulsion and osteochondritis dissecans tend to involve the adolescent athlete.⁶ The term “little league

elbow” was coined in 1960 by Brogden to describe a medial epicondyle fracture in an adolescent pitcher.²⁷ Since that time the term has been associated with several additional injuries to the elbow and is now best avoided altogether.

The medial epicondyle is the weakest structure of the immature elbow. Children may present with apophysitis, often shown radiographically by increased density or even fragmentation of the ossification center.²⁸ Comparison with the contralateral elbow may be helpful to assess subtle changes in size, appearance, or displacement from the humeral condyle.²⁸ This is the last ossification center to fuse with the distal humerus,²⁹ usually in the mid to late teens. Avulsion injury then becomes more common as



Figure 10 Evaluation of articular injury. (A) Lateral radiograph reveals intraarticular ossified fragment (white arrow) and suspected articular defect along anterior margin of radial head (black arrow). (B) Reformatted sagittal CT image confirms and more fully defines fractured radial articular donor site (black arrow). Free fragment is also partially imaged on this selected image slice (white arrow). (C) Anteroposterior view in a different patient reveals articular defect of medial radial head (black arrowhead) and faint triangular loose body in lateral joint recess (white arrowhead). Radiographic visibility of such osteochondral fractures depends on presence of subcartilaginous bone. (D) Coronal T2-weighted MR image with fat-saturation best shows extent of injury. Both cartilaginous and osseous components of displaced and rotated osteochondral fragment are well seen (arrow). Donor site and remaining radial articular surface is also nicely characterized for presurgical planning.

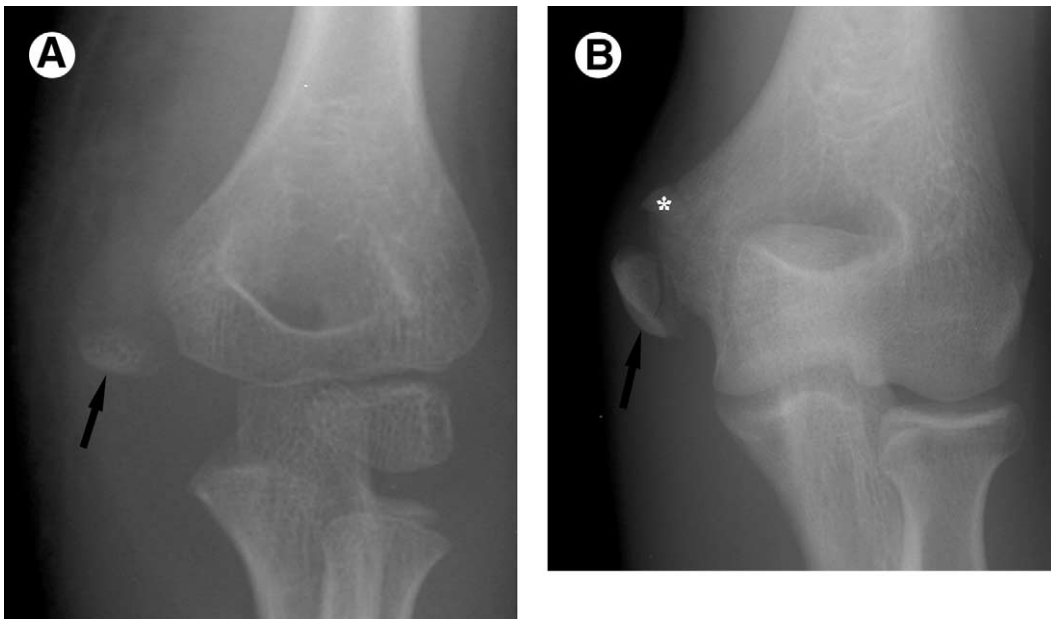


Figure 11 Medial injuries in the young athlete. (A) Anteroposterior view in young child shows avulsion of medial epicondyle ossification center. Displacement of at least 1 centimeter or incarceration within joint is indication for surgical fixation. (B) Anteroposterior view in older child demonstrates Salter–Harris-type III fracture through medial epicondylar epiphysis and physis. Fracture fragment (arrow) is displaced approximately 1.5 cm from the intact proximal epiphyseal component (asterisk).

muscle strength also increases (Fig. 11). Importantly, the avulsed fragment may become significantly displaced and incarcerated within the joint, an absolute indication for open reduction and internal fixation of the fracture. This injury pattern may be missed in younger children if the displaced medial epicondyle is mistaken for the trochlear epiphysis, which does not ossify until the ninth or tenth year.³⁰

The compressive and shear forces across the radiocapitellar joint may lead to osteochondral injury. Osteochondritis dissecans (OCD) of the capitellum presents most commonly, followed by OCD of the radial head. Chronic repetitive microtrauma is felt to lead to a focal ischemic necrosis within the subchondral bone, which goes on to collapse.² Unstable lesions may fragment or become displaced and are a significant cause of permanent elbow disability in young athletes.⁸ Early imaging with radiographs will show subtle focal flattening or subarticular radiolucency along the anterior capitellar margin (Fig. 12).^{2,31} MR imaging with cartilage-sensitive sequences or MR arthrography can help determine the size and stability of the lesion, condition of overlying cartilage, presence of loose bodies, and the condition of the radial head (Fig. 12B).^{1,8,32} This disease entity should be differentiated from Panner's disease (Fig. 12D), osteochondrosis of the capitellum, which typically presents in a younger population.^{33,34} Although a common cause of chronic lateral elbow pain in athletes under the age of 10, this process is self-limited and usually resolves with rest. Global, rather than focal, involvement of the capitellum is characteristic and loose body formation is rare.³⁵ Ossified components of

the intact cartilage of the capitellum undergo fragmentation, resorption, and reossification, often with no residual articular deformity.^{2,25,31}

In addition to medial tensile and lateral compressive forces, a shearing stress is applied to the olecranon during throwing. This stress may lead to apophysitis or avulsion of the olecranon ossification center in children. Adolescent and young adult athletes may develop marginal osteophyte formation along the posteromedial olecranon, stress fracture, or even complete fracture of the olecranon process (Fig. 13).^{6,36} Nonunion and the formation of posterior loose bodies are common complications in the absence of early surgical fixation.³⁶

Tendon Ruptures

The most common tendon ruptures of the elbow involve the biceps and triceps tendons. Biceps tendon tear may occur at the origin of the long head of the biceps tendon, superior glenoid tubercle, or at its attachment to the radial tuberosity. The former injury commonly occurs in the elderly and is associated with rotator cuff tear. The latter injury tends to occur in the dominant arm of active men as a result of sudden loading, such as in lifting or catching a heavy object. On lateral radiograph of elbow, a complete distal biceps rupture is manifested by proximal retraction of the muscle belly, giving a "Popeye-the-sailor-man" (cartoon character from the 1950s) appearance (Fig. 14A and B). A fleck of bone may be seen proximal to the radial tuberosity. On lateral radiograph, triceps tendon rupture is diagnosed when there is an avulsion of the olecranon tip

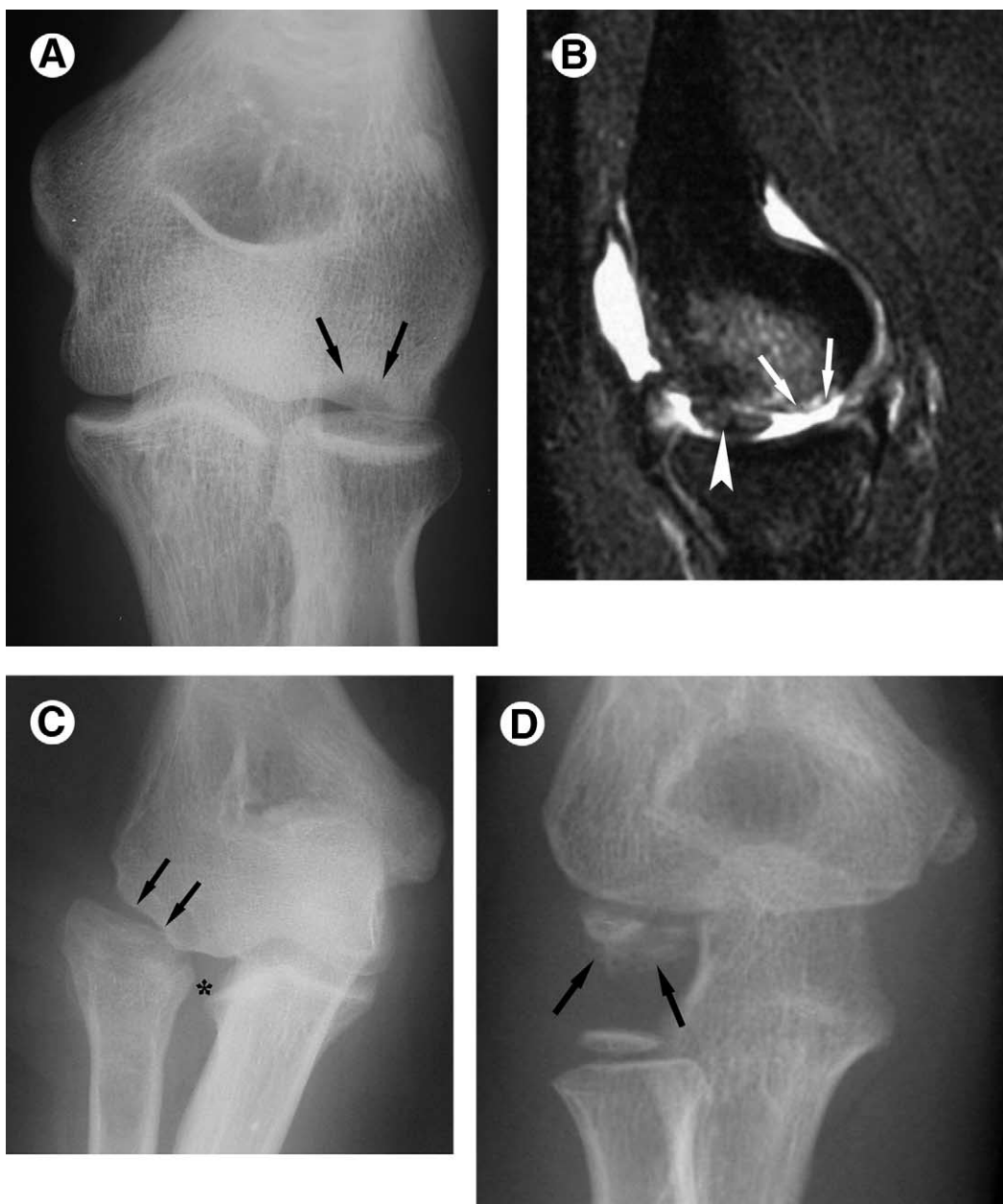


Figure 12 Lateral injuries in young athlete. (A) Anteroposterior view in adolescent pitcher with elbow pain demonstrates subtle subarticular lucency involving capitellum (arrows). This finding represents early radiographic changes of osteochondritis dissecans. (B) Sagittal T2-weighted MR image with fat-saturation shows changes of advanced osteochondritis dissecans in different patient. Partially ossified free capitellar fragment is seen posteriorly displaced (arrowhead) as well as irregular partial-thickness cartilage denudation of anterior articular surface (arrows). (C) Anteroposterior view in different patient demonstrates chronic changes of untreated osteochondritis dissecans. Note deformed articular surfaces of both capitellum (arrows) and radial head. In addition, there is lateral subluxation of radial head and widening of proximal radioulnar joint (asterisk) in this patient with clinical rotatory instability. Chronic instability is common following loss of elbow joint congruency. (D) Anteroposterior view shows typical appearance of Panner's disease, osteochondrosis of capitellum, in a young gymnast. The entire capitellum ossification center appears mottled (arrows). This entity, appearing in the younger age group, should be distinguished from osteochondritis dissecans. Global, rather than focal, involvement of capitellum is usual; symptoms are self-limited, and complete clinical and radiographic resolution are expected.

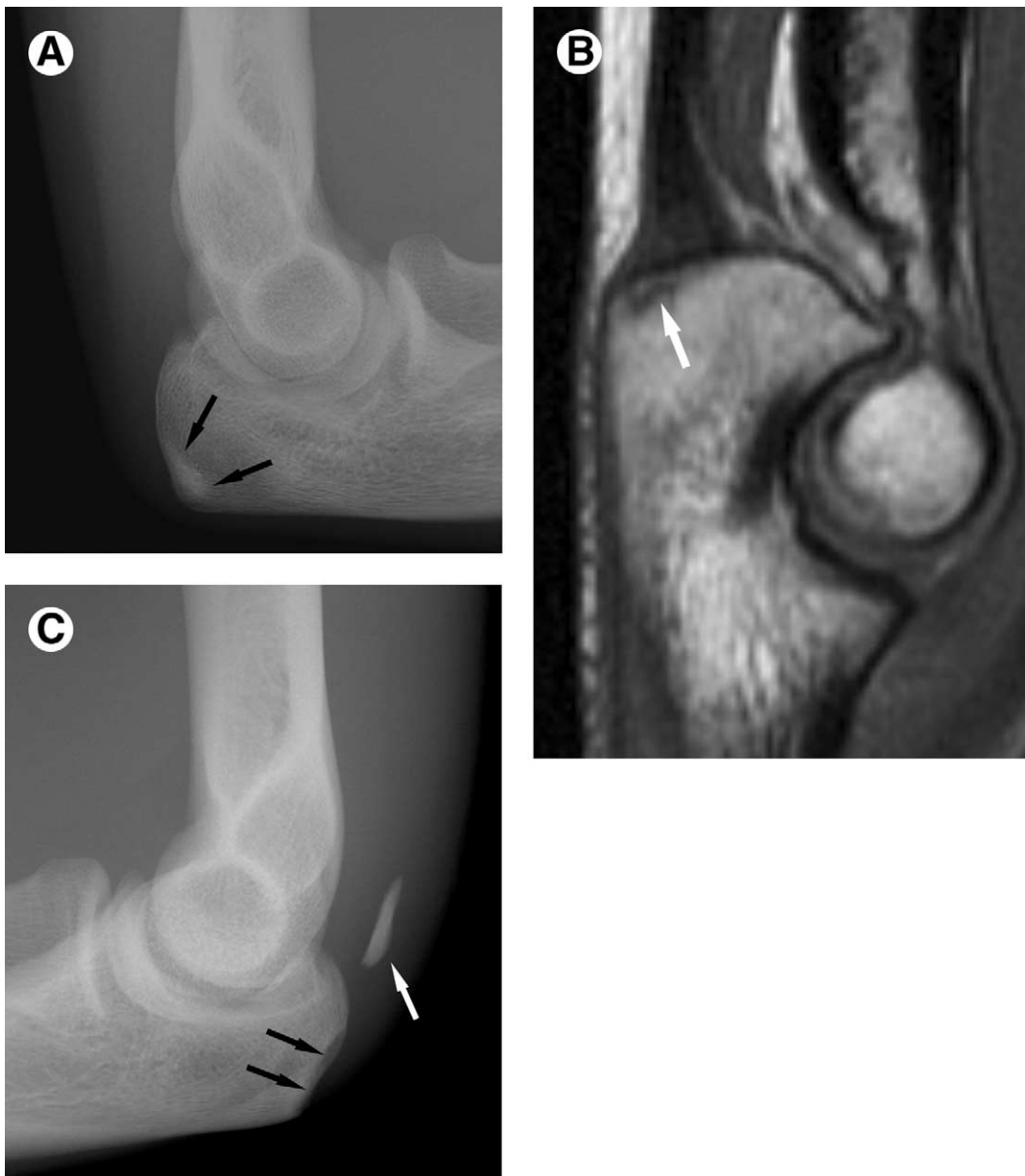


Figure 13 Posterior injuries of the young athlete. (A) Lateral view shows focal linear area of sclerosis along posterior border of olecranon process (arrows) in young throwing athlete with posterior pain. (B) Sagittal T1-weighted MR image confirms stress fracture in this location. Small serpentine hypointense line (arrow) interrupts hyperintense bone marrow in region of fracture. (C) Lateral radiograph in different young pitcher demonstrates displaced avulsion fracture (white arrow) of olecranon process (black arrows). Complete fracture is not uncommon at site of chronic stress change in young athletes.



Figure 14 Tendon ruptures. (A) Lateral radiograph of elbow shows focal bulge of biceps muscle (white arrow). (B) Sagittal T1-weighted MRI shows retracted biceps tendon (white arrow). (From Chew FS: *The Core Curriculum: Musculoskeletal Imaging*. Philadelphia, PA: Lippincott Williams & Wilkins, 2003, with permission) (C) Lateral radiograph of elbow reveals calcification and soft-tissue swelling (white arrow) within course of triceps muscle. (D) Sagittal STIR MR image shows retracted triceps tendon (arrow) and bone marrow edema in olecranon process (arrowhead). Images contributed by Liem T. Bui-Mansfield, Brooke Army Medical Center, San Antonio, TX.

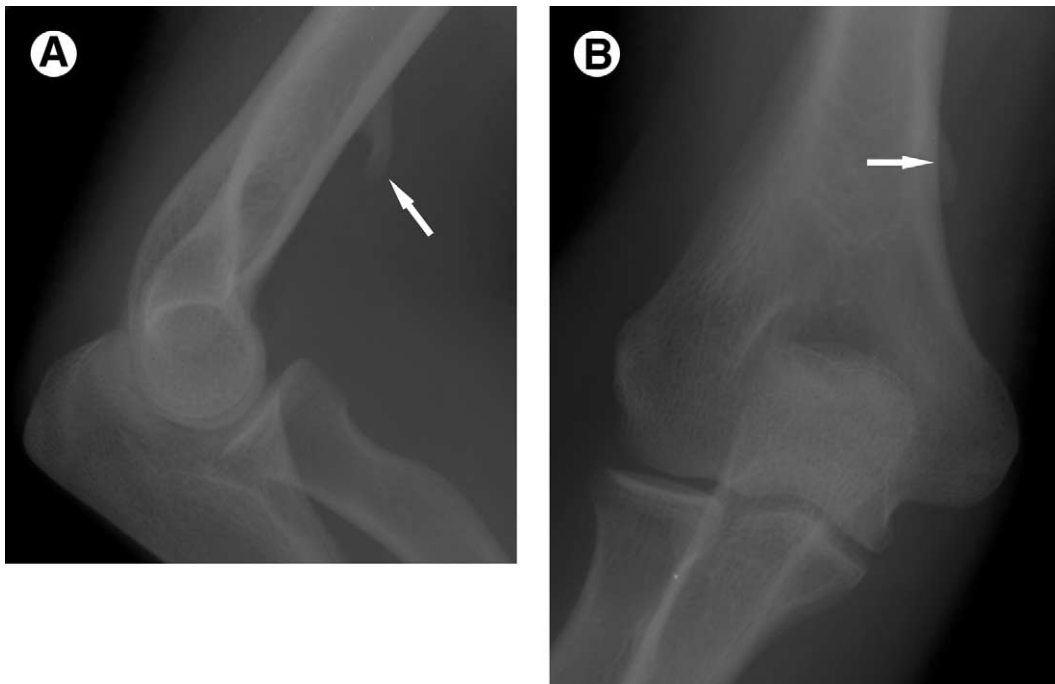


Figure 15 Supracondylar process. (A) Lateral and (B) anteroposterior views demonstrate ossified process (white arrows) extending off distal humeral anteromedial cortical surface. Entrapment syndromes may result from ligamentous bridging between process and humeral medial epicondyle.

at the attachment site of the triceps tendon, which is wavy and edematous (Fig. 14C and D). Both biceps and triceps tendon ruptures are best demonstrated on sagittal T2-weighted sequence.

Supracondylar Process

Sir John Struthers in 1854 first described a bony projection extending off the anteromedial aspect of the humerus, approximately 5 to 6 cm proximal to the epicondyle. This supracondylar process (or avian spur) may be seen in approximately 2% of the population and is usually clinically silent. Occasionally a ligamentous attachment between the spur and the medial epicondyle (ligament of Struthers) may lead to symptomatic compression of the traversing median nerve or brachial artery.^{37,38} The anteroposterior and lateral radiographic views will best demonstrate the bony spur (Fig. 15), which should not be confused with an osteochondroma. The latter often points away from its adjacent joint and will show contiguity with the underlying humeral medullary bone. The humeral cortex remains intact beneath the supracondylar process.³⁸

Loose Bodies

The elbow is second only to the knee in incidence for the development of intraarticular loose bodies, which derive from the cartilage-covered articular surfaces and synovial membranes of joints. These fragments may be chondral, osseous, or osteochondral, and are a common cause of intermittent joint locking, pain, effusion, and secondary osteoarthritis (Fig. 16).³⁹ The bodies may remain free-floating or become adherent to the synovium.⁴⁰ Occasion-

ally, when sequestered within a joint recess or bursa, the loose bodies may be asymptomatic. Most cases of single loose body formation are secondary to acute or chronic trauma with associated osteochondral injury. The presence of multiple fragmented bodies is more suggestive of osteoarthritis and osteonecrosis. A primary form of synovial osteochondromatosis describes the creation of loose bodies within synovium that has undergone chondro-osseous metaplasia (Fig. 17).^{39,40} Multiple bodies of uniform size and variable ossification are characteristic of this entity.

Loose bodies must be at least partially mineralized to become radiographically apparent. Routine elbow films will underestimate the presence of chondral fragments or secondary damage to the articular surfaces.³⁹ In addition, loose bodies tend to collect in the anterior and posterior joint recesses of the elbow. The coronoid and olecranon fossae may hide or obscure loose bodies on routine projections. MR imaging and MR arthrography are sensitive techniques in detecting the type and number of intraarticular bodies, as well as evaluating the articular surfaces and synovium. Axial and sagittal T2-weighted MR sequences are most sensitive in the detection of intraarticular loose bodies. CT, especially with recent advances in volumetric acquisition and multiplanar data reformation, allows confident localization of partially or minimally ossified fragments. The multiplanar and dynamic capability of ultrasound, though highly operator dependent, is becoming more widely utilized in the evaluation of intraarticular bodies.^{2,23}

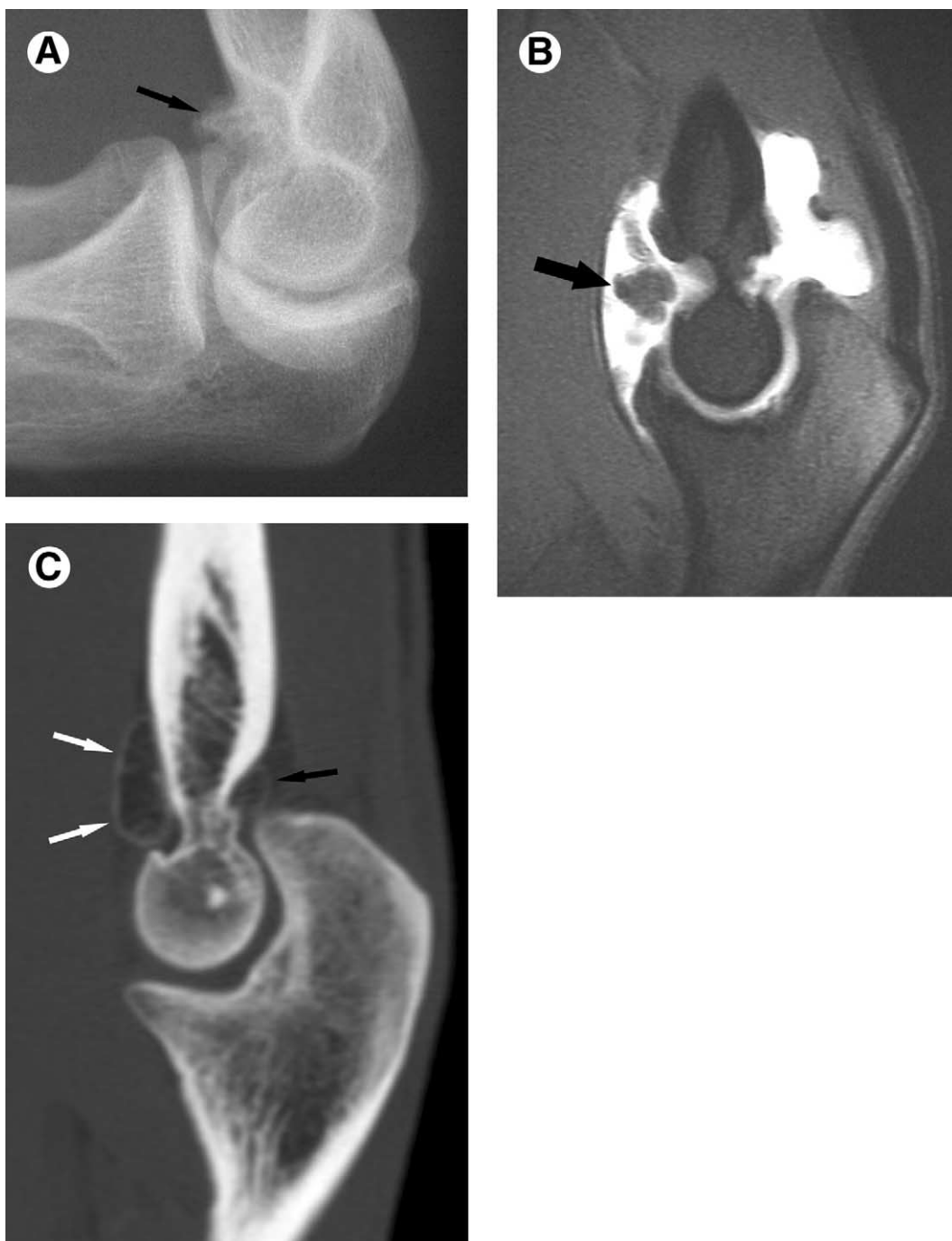


Figure 16 Loose bodies. (A) Lateral radiograph reveals calcified body in region of the coronoid recess (arrow). (B) Sagittal T1-weighted MR arthrogram image with fat saturation confirms presence and location of intraarticular body (arrow). This technique enjoys high sensitivity in detection of loose bodies and is helpful in distinguishing true loose bodies from those sequestered within synovium or adjacent bursa. (C) Sagittal reformatted CT image in different patient demonstrates ossified bodies within anterior (white arrows) and posterior (black arrow) joint recesses. Posterior loose body was occult radiographically.



Figure 17 Synovial osteochondromatosis. (A) Anteroposterior view shows ill-defined mineralization within proximal radioulnar joint. (B) Axial CT image through this level confirms presence of multiple small ossified bodies within joint space and bicipitoradial bursa (arrows). This appearance results from primary chondro-osseous metaplasia of synovium and with synovectomy. (C) Lateral radiograph in different patient demonstrates multiple irregular ossified bodies within anterior and posterior joint recesses (arrows) and distension of olecranon bursa (asterisk), which is commonly seen in primary synovial disorders. (D) Sagittal T2-weighted MR image reveals multiple, predominantly hypointense intraarticular bodies. Some of these bodies demonstrate hyperintense cartilaginous margins (arrows). This appearance is typical of synovial osteochondromatosis.

Enthesopathy and Calcific Tendinopathy

Reactive bone changes may occur at tendinous insertion sites about the elbow. These changes may be minimal, such as along the medial and lateral epicondyles at the insertions of the common flexor and extensor tendons (Fig. 18A), or may develop into discreet projections as are

often seen at the insertion of the triceps brachii on the olecranon process (Fig. 18B).⁴¹

The deposition of calcium hydroxyapatite within periarticular soft tissues, predominantly tendons, is commonly referred to as calcific tendinopathy. This entity presents radiographically as dense, amorphous, or cloud-like

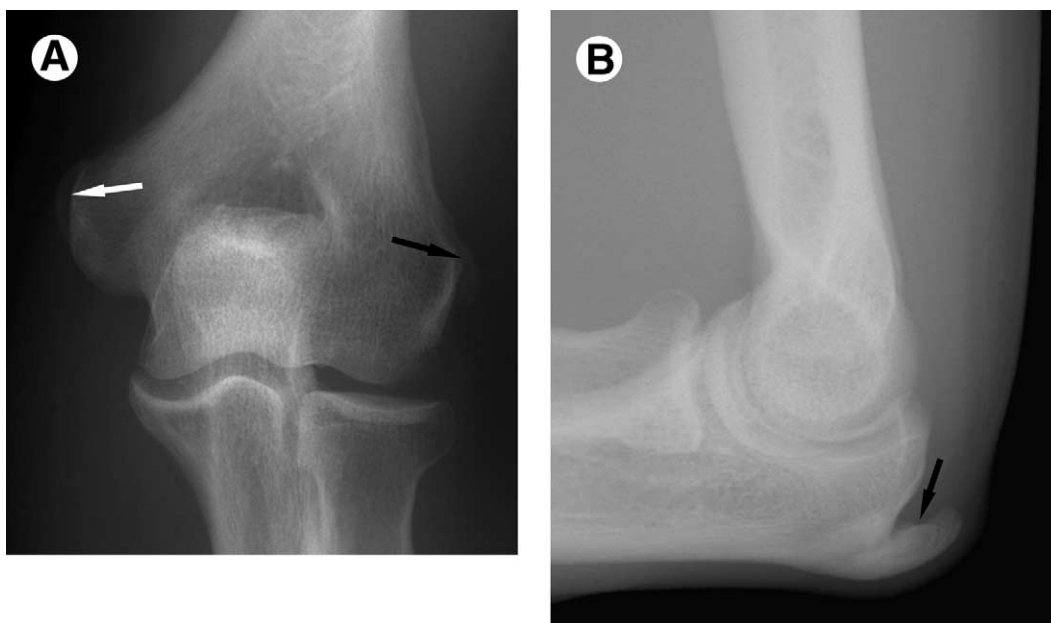


Figure 18 Enthesopathy. (A) Anteroposterior view demonstrates enthesophyte development along medial (white arrow) and lateral (black arrow) epicondyles. These changes occur at insertion sites of common flexor and extensor tendons, respectively. (B) Lateral radiograph in different patient reveals large enthesophyte (arrow) extending from posterior margin of olecranon process, at site of insertion of triceps brachii tendon.

calcific foci and tends to occur in regions of necrosis and mucoid degeneration.⁴² Patients who present with symptoms of epicondylitis often demonstrate faint calcification along the epicondylar margins (Fig. 19A).⁴³ Dystrophic calcification within the relatively hypoxic distal triceps brachii tendon is also commonly seen (Fig. 19B). Hydroxyapatite crystal deposition may persist, progress in size, or spontaneously resolve with or without recurrence.⁴⁴ Serial examinations showing newly displaced foci suggest rupture and retraction of the involved tendon. On MR imaging, there may be associated bone marrow edema adjacent to the site of calcific tendonitis that may mimic tumor or infection.⁴⁵

Rheumatoid Arthritis

Rheumatoid arthritis is an idiopathic inflammatory disease of the synovium, which presents as a symmetric inflammatory arthropathy (Fig. 20). The elbow is affected in 50% of patients with rheumatoid arthritis⁴⁶ and follows a slower course of cartilage destruction than the larger weight-bearing joints of the hip and knee.⁴⁷ Radiographic hallmarks of this disease include early marginal erosions along the bare areas of the joint (Fig. 20C and D) and eventual uniform narrowing of the joint space as articular cartilage is lost.^{47,48} Joint effusion with displacement of the fat pads, olecranon bursitis, and subcutaneous rheumatoid nodules may be evident during active disease. With advanced disease, large subarticular cysts may form and continued articular destruction leads to mechanical instability (Fig. 20E). Characteristic thinning of the olecranon process and proximal deepening of the trochlea in end-stage disease allow posterior migration of the proximal

ulna beneath the humerus (Fig. 20F).⁴⁹ Table 3 is a summary of the radiologic features of rheumatoid arthritis.

Olecranon Bursitis

The olecranon bursa forms between the olecranon process and the superficial subcutaneous tissues after early childhood.⁵⁰ Fluid distension of this region represents the most common site of superficial bursitis and is easily confirmed radiographically with careful study of the soft tissues on lateral radiographs (Fig. 21). Fusiform soft-tissue swelling and subtle increased radiodensity will be seen. Occasionally, depending on the etiology of bursal inflammation, loose bodies or calcium deposition will be evident. The causes of olecranon bursitis are myriad and include traumatic, overuse (student's elbow), inflammatory, and infectious processes.⁵¹ Common inflammatory processes include rheumatoid arthritis, gout, calcium pyrophosphate deposition, hydroxyapatite crystal deposition, and xanthoma.⁵² When bilateral, this condition is highly suggestive of gout.

Hemophilia

Chronic hemarthritis may occur in patients with bleeding disorders and commonly involves the knees, ankles, and elbow joint. Blood within the joint irritates the synovium, which then undergoes villous hypertrophy and becomes friable.⁵³ Thus, a vicious cycle ensues whereby additional bleeding may occur. In the young patient, the epiphyseal growth plates hypertrophy (Fig. 22A) and may ossify prematurely, and angular deformities occasionally result. Continued bleeding into adulthood destroys articular car-

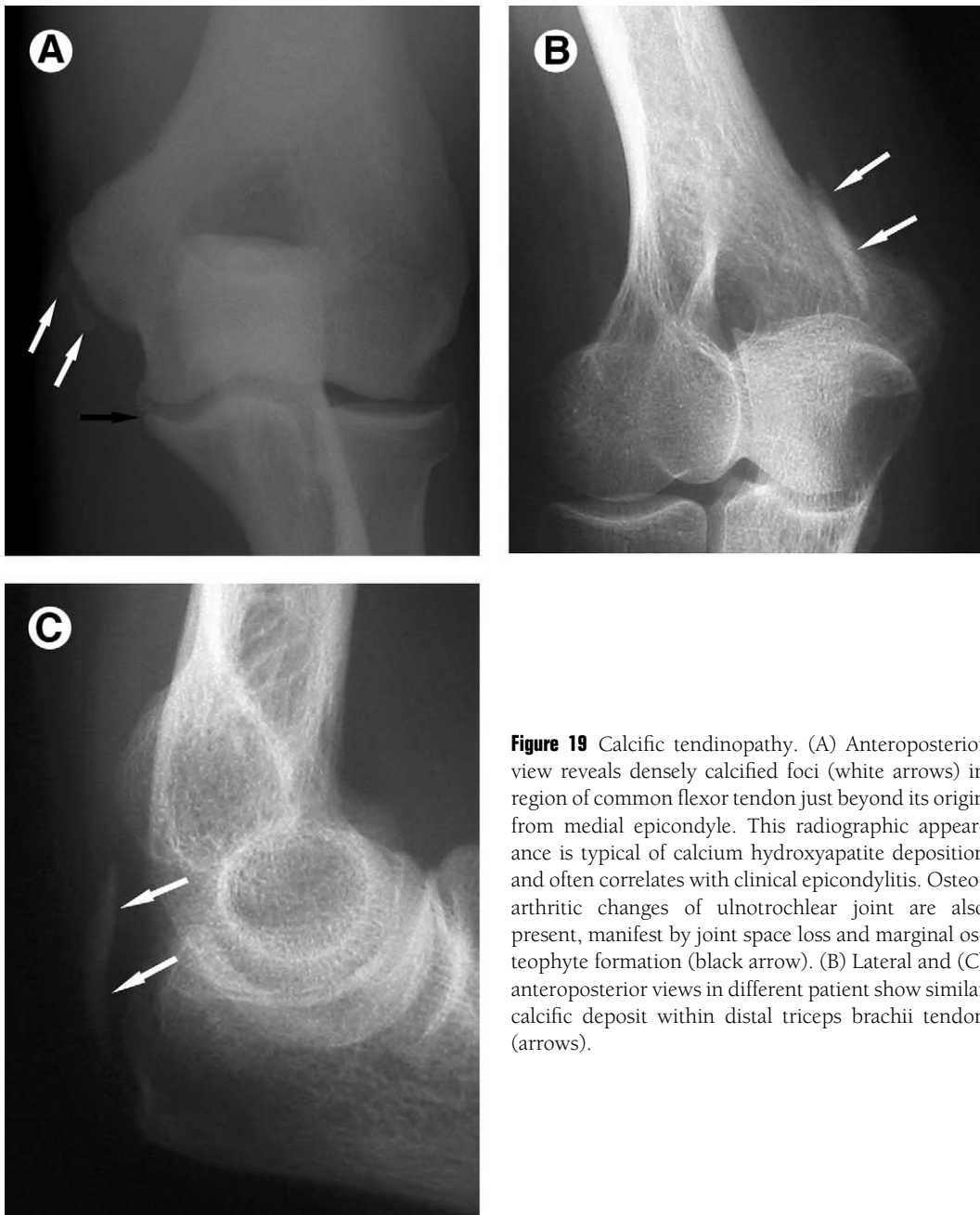


Figure 19 Calcific tendinopathy. (A) Anteroposterior view reveals densely calcified foci (white arrows) in region of common flexor tendon just beyond its origin from medial epicondyle. This radiographic appearance is typical of calcium hydroxyapatite deposition and often correlates with clinical epicondylitis. Osteoarthritic changes of ulnotrochlear joint are also present, manifest by joint space loss and marginal osteophyte formation (black arrow). (B) Lateral and (C) anteroposterior views in different patient show similar calcific deposit within distal triceps brachii tendon (arrows).

Figure 20 Rheumatoid arthritis. (A) Lateral radiograph shows large dense effusion of elbow joint in patient with early active rheumatoid arthritis. Posterior fat pad is visible (black arrow); anterior fat pad is displaced (white arrow) and periradial recess is distended (arrowhead). Articular surfaces appear normal. (B) Axial T2-weighted MR image with fat saturation through level of periradial recess in same patient as (A) is shown. There is distension of joint capsule (arrows) with underlying isointense synovial pannus formation. (C) Anteroposterior view in different patient with more advanced disease demonstrates uniform loss of radiocapitellar joint (black arrows), marginal erosion of ulnotrochlear joint (white arrows), and erosion of ulnar aspect of proximal radioulnar joint (arrowhead). (D) Axial T1-weighted MR image through level of the proximal radioulnar joint in same patient as (C) shows location and degree of marginal erosive changes (arrows) to better advantage than does radiography. (E) Lateral view in different patient with rheumatoid arthritis. Presence of joint effusion (white arrowhead), uniform loss of joint space, marginal erosive change (black arrow), and subchondral cyst formation (white arrow) are all typical features of advanced disease. Secondary osteoarthritic changes may become superimposed, as in this case with marginal osteophyte formation along anterior ulnotrochlear joint (black arrowhead), especially once the inflammatory component is no longer active. (F) Lateral radiograph demonstrates end-stage changes of rheumatoid arthritis. Olecranon process is extremely thinned with widening of trochlear groove (arrows). Ulna then translates posteriorly, due to inherent instability of hinge mechanism, allowing radial head (asterisk) to subluxate anteriorly and proximally into humerus.

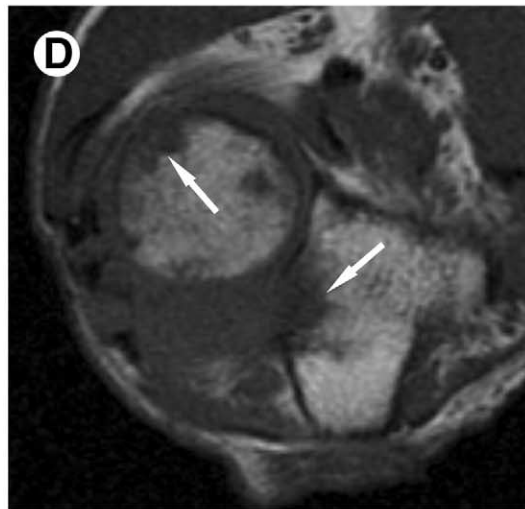
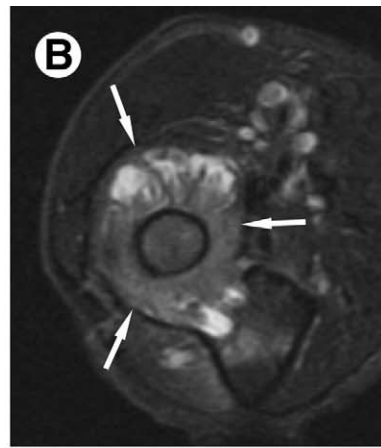
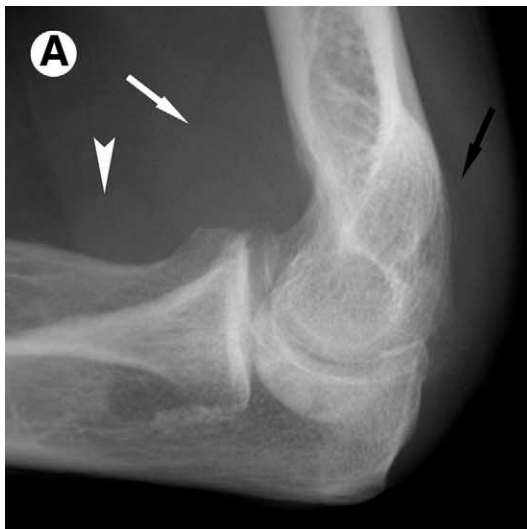


Table 3 Radiologic Features of Rheumatoid Arthritis

Periarticular osteoporosis progressing to generalized osteoporosis
Fusiform periarticular soft tissue swelling
Uniform loss of joint space
Marginal erosions progressing to severe erosions of subchondral bone
Synovial cyst formation
Subluxations
Lack of reactive bone formation [distinguish it from seronegative spondyloarthritis]
Bilateral symmetric distribution
Distribution: hands (MCPJ, PIPJ), feet, knees, hips, upper cervical spine, shoulder, and elbows, in decreasing order of frequency

MCPJ = metacarpophalangeal joint; PIPJ = proximal interphalangeal joint.

Adapted from Brower AC. *Arthritis in Black and White* (ed 2). Philadelphia, PA, WB Saunders, 1997.

tilage. Radiographically this is shown by loss of joint space, subchondral cyst formation, and often the presence of a dense joint effusion (Fig. 22B and C). Enlargement of the radial notch of the ulna and of the olecranon fossa are characteristic late changes affecting the elbow.⁵³ Table 4 is a summary of the radiologic features of hemophilic arthropathy.

Heterotopic Ossification

Heterotopic ossification refers to the formation of mature bone within nonosseous tissues. This may occur within inflamed muscle (myositis ossificans) (Fig. 23A)⁵⁴ or supporting ligaments (Fig. 23B), but is most often seen within the joint capsule following traumatic dislocation, surgery,

Table 4 Radiologic Features of Hemophilia

Radiodense soft tissue swelling
Osteoporosis — juxtaarticular or diffuse
Overgrown or ballooned epiphyses
Subchondral cysts
Pseudotumor
Late uniform joint space loss
Late secondary osteoarthritic changes
Asymmetrical sporadic distribution
Distribution in knee, elbow, ankle, hip, and shoulder, in decreasing order; changes distal to the elbow or ankle are rare

Adapted from Brower AC. *Arthritis in Black and White* (ed 2). Philadelphia, PA, WB Saunders, 1997.

burn, or neural axis trauma (Fig. 23C-E).^{55,56} Interestingly, up to 50% of elbow dislocations will form bone in the periarticular tissues.⁵⁷ Ossification of the soft tissues may eventually lead to complete ankylosis of the elbow and usually appears within 3 to 4 weeks of injury.⁵⁸ Rarely this process can engulf the distal biceps tendon or present as compression syndromes with involvement of the median or ulnar nerves.⁵⁵ The radiographic appearance of mature ossified bone should be distinguished from amorphous cloud-like features of calcium hydroxyapatite crystal deposition. Although initially having indistinct margins, heterotopic ossification develops into well-defined trabeculated bone.⁵⁵

Conclusion

Conventional radiography remains an essential initial test in the evaluation of the elbow and its disorders. One must be familiar with the pertinent anatomy, early developmen-

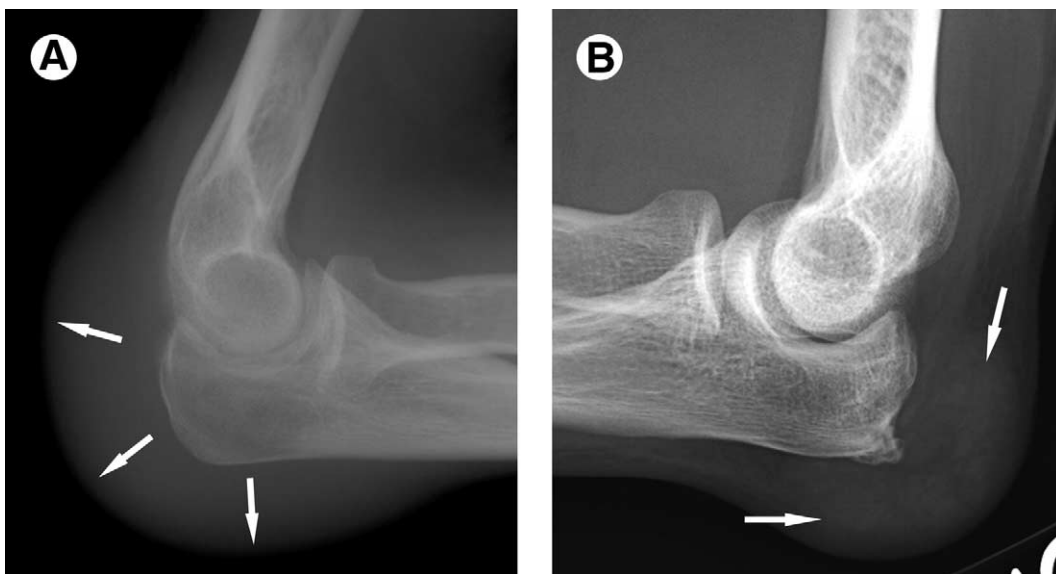


Figure 21 Olecranon bursitis. (A) Lateral view shows marked soft-tissue prominence (arrows) overlying olecranon process in patient with clinical bursitis. (B) Lateral view in different patient reveals reticulated increased densities within inflamed bursa (arrows). This represents mineralization by calcium salts, often seen in association with gout and other crystal deposition disorders.

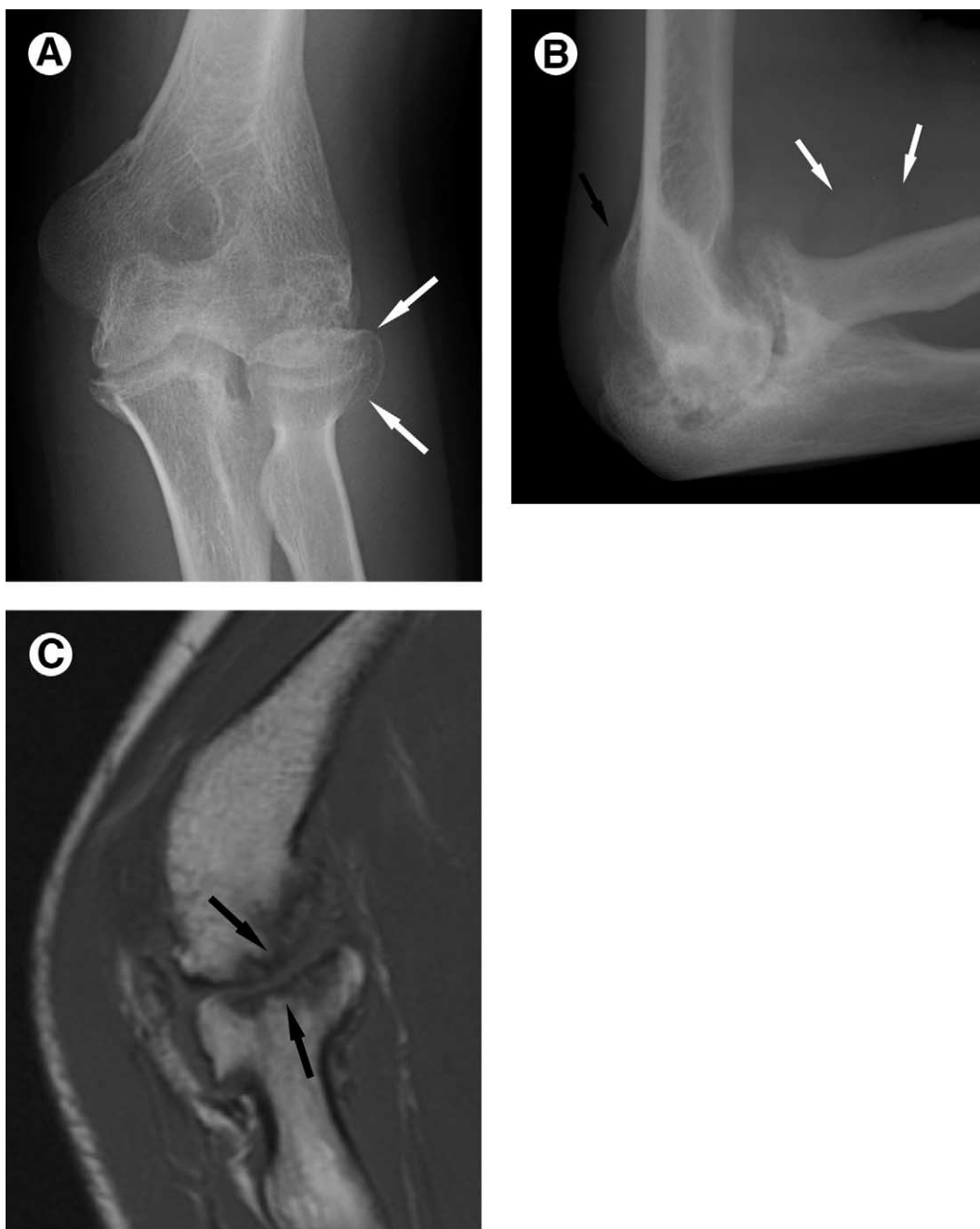


Figure 22 Hemophilia. (A) Anteroposterior view in young person demonstrates overgrowth of radial head (arrows) and early irregularity of ulnotrochlear and radiocapitellar joint surfaces. (B) Lateral radiograph in same patient, 2 years later, reveals more advanced destruction of articular surfaces and formation of subarticular cysts. There is a positive posterior fat pad sign (black arrow) and dense joint effusion with distension of periradial recess (white arrows), suggesting hemarthrosis. (C) Sagittal T1-weighted MR image shows complete loss of cartilage along radiocapitellar joint with irregular sclerosis of subarticular trabecular bone (arrows).



Figure 23 Heterotopic ossification. (A) Anteroposterior view demonstrates characteristic appearance of myositis ossificans. Mass adjacent to distal medial humerus has undergone mature ossification with well-developed peripherally calcified margin (arrows). This appearance should not be confused with central or ill-defined mineralization often associated with primary osseous sarcomas. (B) Anteroposterior view reveals multiple foci of heterotopic ossification at the site of previous surgical repair of radial collateral ligament. (C) Lateral view in different patient 4 weeks following traumatic dislocation of elbow. Ill-defined mineralization is seen along capsular margin (arrows). (D) Lateral view in same patient as (C) several months later shows extensive, matured, ossification of joint capsule. (E) Lateral radiograph in different patient with remote history of elbow dislocation shows near complete bony ankylosis of elbow joint and osseous encapsulation of distal biceps brachii tendon (asterisk).

tal changes, and the biomechanics of this complex joint to appreciate subtle injury patterns and articular disorders. In some cases, radiographic imaging will point to the need for further evaluation with CT, MR, or sonographic imaging.

References

- Potter HG: Imaging of posttraumatic and soft tissue dysfunction of the elbow. *Clin Orthop* 370:9-18, 2000
- Miller TT: Imaging of elbow disorders. *Orthop Clin North Am* 30:21-36, 1999
- Craig JG, Jacobson JA, Moed BR: Ultrasound of fracture and bone healing. *Radiol Clin North Am* 37:737-751, 1999
- Morrey BF: Anatomy of the elbow joint, in Morrey BF (ed): *The Elbow and Its Disorders* (ed 3). Philadelphia, PA, Saunders, 2000, pp 13-60
- Peterson HA: Physeal injuries of the distal humerus. *Orthopedics* 15:799-808, 1992
- Cain EL Jr, Dugas JR, Wolf RS, et al: Elbow injuries in throwing athletes: a current concepts review. *Am J Sports Med* 31:621-635, 2003
- Berquist TH: Diagnostic imaging of the elbow, in Morrey BF (ed): *The Elbow and Its Disorders* (ed 3). Philadelphia, PA, Saunders, 2000, pp 84-101
- Sofka CM, Potter HG: Imaging of elbow injuries in the child and adult athlete. *Radiol Clin North Am* 40:251-265, 2002
- Norell HG: Roentgenologic visualization of the extracapsular fat: its importance in the diagnosis of traumatic injuries to the elbow. *Acta Radiol* 42:205-210, 1954
- Goswami GK: The fat pad sign. *Radiology* 222:419-420, 2002
- Major NM, Crawford ST: Elbow effusion in trauma in adults and children: is there an occult fracture? *AJR Am J Roentgenol* 178:413-418, 2002
- Bohrer SP: The fat pad sign following elbow trauma: its usefulness and reliability in suspecting "invisible" fractures. *Clin Radiol* 21:90-94, 1970
- Hoffman AD, Graviss ER: Imaging of the pediatric elbow, in Morrey BF (ed): *The Elbow and Its Disorders* (ed 3). Philadelphia, PA, Saunders, 2000, pp 155-163
- Leet AI, Young C, Hoffer MM: Medial condyle fractures of the humerus in children. *J Pediatr Orthop* 22:2-7, 2002
- Rogers LF: The elbow and forearm, in Rogers LF (ed): *Radiology of Skeletal Trauma* (ed 2). New York, NY, Churchill Livingstone, 1992, pp 751-754
- Kuntz DG Jr, Baratz ME: Fractures of the elbow. *Orthop Clin North Am* 30:37-61, 1999
- Morrey BF: Radial head fracture, in Morrey BF (ed): *The Elbow and Its Disorders* (ed 3). Philadelphia, PA, Saunders, 2000, pp 341-364
- Greenspan A, Norman A: The radial head, capitellum view: Useful technique in elbow trauma. *AJR Am J Roentgenol* 138:1186-1188, 1982
- Plancher KD, Lucas TS: Fracture dislocations of the elbow in athletes. *Clin Sports Med* 20:59-76, 2001
- Regan WD, Morrey BF: Coronoid process and Monteggia fractures, in Morrey BF (ed): *The Elbow and Its Disorders* (ed 3). Philadelphia, PA, Saunders, 2000, pp 396-408
- Essex-Lopresti P: Fractures of the radial head with distal radio-ulnar dislocation: report of two cases. *J Bone Joint Surg Br* 33:244-247, 1951
- Regan WD, Morrey B: Fractures of the coronoid process of the ulna. *J Bone Joint Surg Am* 71:1348, 1989
- Frankel DA, Bargiela A, Bouffard JA, et al: Synovial joints: Evaluation of intraarticular bodies with US. *Radiology* 206:41-44, 1998
- Beltan J, Rosenberg ZS, Kawelblum M, et al: Pediatric elbow fractures: MRI evaluation. *Skeletal Radiol* 23:277-281, 1994
- Hutchinson MR, Ireland ML: Overuse and throwing injuries in the skeletally immature athlete. *Instr Course Lect* 52:25-36, 2003
- Wilson FD, Andrews JR, Blackburn TA, et al: Valgus extension overload in the pitching elbow. *Am J Sports Med* 11:83-88, 1983
- Brogden BS, Crow MD: Little leaguer's elbow. *AJR Am J Roentgenol* 83:671-675, 1960
- Klinge KE, Mininder SK: Little league elbow: valgus overload injury in the paediatric athlete. *Sports Med* 32:1005-1015, 2002
- Silberstein MJ, Brodeur AE, Graviss ER, et al: Some vagaries of the medical epicondyle. *J Bone Joint Surg Am* 63:524, 1981
- el-Khoury GY, Daniel WW, Kathol MH: Acute and chronic avulsive injuries. *Radiol Clin North Am* 35:747-766, 1997
- Takahara M, Ogino TM, Takagi M, et al: Natural progression of osteochondritis dissecans of the humeral capitellum: initial observation. *Radiology* 216:207-212, 2000
- Fritz R: MR imaging of osteochondral and articular lesions. *Magn Reson Imaging Clin N Am* 5:579-602, 1997
- Bradley JP, Petrie RS: Osteochondritis dissecans of the humeral capitellum. Diagnosis and treatment. *Clin Sports Med* 20:565-590, 2001
- Schenck JR, Goodnight JM: Osteochondritis dissecans. *J Bone Joint Surg Am* 78:439-456, 1996
- Panner HJ: A peculiar affection of the capitellum humeri, resembling Calve-Perthes disease of the hip. *Acta Radiol* 10:234-242, 1929
- Nuber GW, Diment MT: Olecranon stress fractures in throwers: a report of two cases and a review of the literature. *Clin Orthop* 278:58-61, 1992
- Al-Qattan MM, Husband JB: Median nerve compression by the supracondylar process: a case report. *J Hand Surg* 16-B:101-103, 1991
- Subasi M, Kesemenli C, Necmioglu S, et al: Supracondylar process of the humerus. *Acta Orthop Belg* 68:72-75, 2002
- Bianchi S, Martinoli C: Detection of loose bodies in joints. *Radiol Clin North Am* 37:679-690, 1999
- Kamineni S, O'Driscoll SW, Morrey BF: Synovial osteochondromatosis of the elbow. *J Bone Joint Surg Br* 84:961-966, 2002
- Resnick D: Degenerative disease of extraspinal locations, in Resnick D (ed): *Bone and Joint Imaging* (ed 2). Philadelphia, PA, Saunders, 1996, pp 321-354
- Hays CW, Conway WF: Calcium hydroxyapatite deposition disease. *Radiographics* 10:1031-1048, 1990
- Pomerance J: Radiographic analysis of lateral epicondylitis. *J Shoulder Elbow Surg* 11:156-157, 2002
- Resnick D: Calcium hydroxyapatite crystal deposition disease, in Resnick D (ed): *Bone and Joint Imaging* (ed 2). Philadelphia, PA, Saunders, 1996, pp 425-436
- Bui-Mansfield LT, Moak M: MR appearance of bone marrow edema associated with hydroxyapatite deposition disease. *J Comput Assist Tomogr* 29:103-107, 2005
- Ljung P, Jonsson K, Rydgren B, et al: The natural course of rheumatoid elbow arthritis: a radiographic and clinical five-year follow up. *J Orthop Rheumatol* 8:32-36, 1995
- Lehtinen JT, Kaarela K, Belt EA, et al: Radiographic joint space in rheumatoid joints. A 15-year prospective follow-up study in 74 patients. *Rheumatology* 40:1141-1145, 2001
- Larsen A, Dale K, Eek M: Radiographic evaluation of rheumatoid arthritis and related conditions by standard reference films. *Acta Radiol* 18:481-491, 1977
- Lehtinen JT, Kaarela K, Kauppi MJ, et al: Bone destruction patterns of rheumatoid elbow: a radiographic assessment of 148 elbows at 15 years. *J Shoulder Elbow Surg* 11:253-258, 2002
- Chen J, Alk D, Eventov I, et al: Development of the olecranon bursa: an anatomic cadaver study. *Acta Orthop Scand* 58:408-409, 1987
- Pien FD, Ching D, Kim E: Septic bursitis: experience in a community practice. *Orthopedics* 14:981-984, 1991
- Morrey BF: Bursitis, in Morrey BF (ed): *The Elbow and Its Disorders* (ed 3). Philadelphia, PA, Saunders, 2000, pp 901-908
- Rodriguez-Merchan EC: Effects of hemophilia on articulation of children and adults. *Clin Orthop* 328:7-13, 1996
- Thompson HC III, Garcia A: Myositis ossificans: aftermath of elbow injuries. *Clin Orthop* 50:129-134, 1967
- Viola RW, Hastings H 2nd: Treatment of ectopic ossification about the elbow. *Clin Orthop* 370:65-86, 2000
- Ilahi OA, Strausser DW, Gabel GT: Post-traumatic heterotopic ossification about the elbow. *Orthopedics* 21:265-268, 1998
- Hildebrand KA, Patterson SD, King GJ: Acute elbow dislocations: simple and complex. *Orthop Clin North Am* 30:63-79, 1999
- Ilahi OA, Bennett JB, Gabel GT, et al: Classification of heterotopic ossification about the elbow. *Orthopedics* 24:1075-1078, 2001